

# Fatigue crack growth behaviour of a Si–Mn steel with carbide-free lathy bainite

LIU WENYAN, QU JINGXIN, SHAO HESHENG

*P.O. Box 67, D11 Xueyuan Road, Beijing Graduate School, CUMT, Beijing 10083, Peoples Republic of China*

An investigation has been performed to examine the fatigue crack propagation (FCP) rate and fatigue threshold of an Si–Mn steel containing carbide-free lathy bainite. Compact tension specimens prepared from this steel were given four different heat treatments to produce four different austenite contents. The fatigue test was carried out at stress ratio of  $-1$  in a room temperature ambient atmosphere. The results show that the FCP threshold of the steel increases with an increase in the volume fraction of carbon-saturated austenite. The crack growth behaviours show that the deformation strengthening ability of the austenite has a significant effect on the FCP in the threshold region. The effect of austenite on the FCP threshold is seven times that of the bainite.

## 1. Introduction

Previous investigations on silicon containing steels have shown that the presence of a high silicon content in low alloy steels, isothermally transformed in the bainitic temperature region, encourages the retention of a large amount of carbon-rich austenite in conjunction with carbide-free bainitic-ferrite. This occurs rather than the formation of brittle interlath cementite films which lead to a detrimental effect on the toughness [1–6]. The bainite has a lath shaped morphology. Its individual ferrite areas are separated by the “thin-film” type of austenite [7–9]. It has a high dislocation density instead of twins [9–11]. This is because silicon significantly retards the precipitation of cementite from the residual austenite during the bainitic transformation.

Subsequent microstructural and property studies [8–15] have indicated that, with this microstructure, these steels display enhanced mechanical properties: an ultrahigh strength, a high toughness and an improved combination of strength and toughness, as compared to the behaviour of these steels in the fully martensitic condition. The carbide-free lathy bainite also has a higher resistance to abrasive wear, impact fatigue and contact fatigue [16–18]. It is also highly versatile with respect to manufacturing. Furthermore, the manufacturing cost of a component is significantly lower than for other ultrahigh strength steels.

When a structural component is subjected to cyclic loading, fatigue crack propagation (FCP) rate properties are of vital importance for structural reliability assessment. Some early studies [19–23] have indicated that, a lower bainitic structure rather than martensitic structure in the same steel, or a bainite (both upper and lower)–martensite mixed microstructure rather than the fully martensitic structure at

nearly the same hardness or strength level, show greater fracture toughness, a higher threshold and better FCP resistance. However, the FCP behaviours and structure–FCP relationships of the lathlike carbide-free bainite has not been reported in the literature. In this study, the FCP rates were obtained over a wide range of  $\Delta$  stress intensity factor levels from the near-threshold crack propagation to the high stress intensity range regimes. The effects of microstructure on the FCP rate and threshold were also investigated.

## 2. Experimental procedure

### 2.1. Materials

The material investigated in this study was a Si–Mn steel. The nominal chemical composition of the steel is 0.6 wt % C–2.3 wt % Si–1.5 wt % Mn–0.6 wt % Cr–0.10 wt % S–0.015 wt % P. The steel was melted in an electric furnace and cut into specimens after forging. These specimens were austenitized at 1163 K for 10 min in a NaCl–KCl salt bath and then quenched into a  $\text{KNO}_3$ – $\text{NaNO}_3$  salt bath set at various temperatures (573, 593, 623, and 643 K). After isothermal holding for 30 min, the specimens were finally quenched into water.

The structures and fractures were observed using a Cambridge-S360 scanning electron microscope (SEM) and a JEM-200CX transmission electron microscope (TEM). The volume fraction of austenite (FA) was measured using an anode-rotating X-ray diffractometer D/Max-ra, using Miller’s technique of rotating and tilting the sample surface about an incident beam of  $\text{CuK}_\alpha$  radiation. The sample surfaces were electropolished in a mixed solution of phosphoric and chromic acids. A scanning speed of  $0.0030^\circ \text{s}^{-1}$  was used and the combination of peaks

chosen for analysis was (200), (211), (200), (220) and (311). The cathode tube voltage was 50 kV and the current was 100 mA.

The microstructures were carbide-free lathy bainite transformed at the given temperatures, as shown in Fig. 1(a–e). The mechanical properties and FA values are presented in Table 1.

### 2.2. Specimen geometry

The FCP rate testing was conducted on compact tensile (CT) specimens. The planar dimensions were 48 mm high, 40 mm wide and 14 mm thick. The ratio of machine notch depth to specimen width was equal to 0.5.

### 2.3. FCP testing

Tests were conducted at ambient temperature in laboratory air using a 40 kN close-loop servo-controlled electrohydraulic Schenck machine operating at a frequency of 30 Hz. Tests at a constant stress intensity factor range ( $\Delta K$ ) and at a constant stress ratio of 0.1 were performed to obtain the FCP behaviour at high  $\Delta K$  levels. Prior to the experiments, a fatigue precrack was introduced at a distance greater than 2 mm from the notch root.

A conventional load-shedding technique was employed as the fatigue threshold conditions were approached. Fatigue cracks were initiated at intermediate  $\Delta K$  levels. Subsequent to this, the load was reduced by  $<10\%$  at each load-shedding step while the crack extension rate was assessed. At each load level, the fatigue crack was allowed to grow a distance of approximately four plastic zone sizes characteristic of the previous load level before crack growth was measured. The  $\Delta K$  value was experimentally defined as the  $\Delta K$  level at which a crack extension rate of  $10^{-11}$  m per cycle was approached.

The crack growth was measured optically at room temperature using a low-powered traveling microscope capable of measuring to 0.1 mm. Scanning electron microscopy was used to quantify the fatigue fracture modes prevalent over a range of  $\Delta K$  levels.

## 3. Results and analysis

### 3.1. Fatigue crack growth behaviour

The FCP rate  $da/dN$  as a function of  $\Delta K$  is presented in Fig. 2 for the four microstructures. The graph of the FCP rate against  $\Delta K$  level highlights three regions of

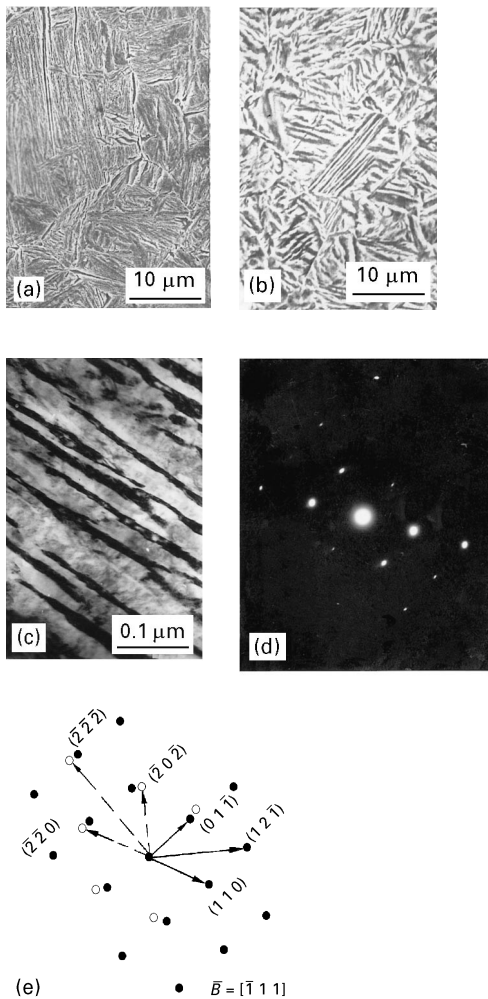


Figure 1 Morphologies of the carbide-free bainite (a) 573 K, SEM (b) 643 K, SEM (c) 573 K, TEM (d) 573 K, Diffraction pattern (e) Pattern index

TABLE I Mechanical properties of the bainitic steel (Heating at 1163 K, salt bath quenching)

Isothermal temperature (K)	HRC	UTS (MPa)	YS (MPa)	EL (%)	RA (%)	FA (%)
573	52	1940	1691	12.4	49.6	8.1
593	49	1796	1587	15.6	56.2	10.2
623	46	1615	1400	17.7	60.5	16.6
643	43	1468	1235	20.1	66.3	22.5

HRC – Rockwell hardness c, UTS – Ultimate tensile strength, YS – Yield strength, EL – Elongation, RA – Reduction in area, FA – Volume fraction of austenite

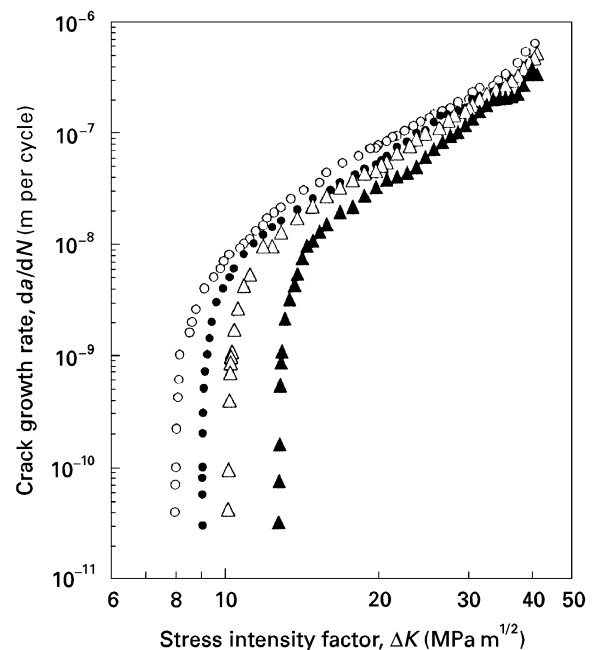


Figure 2 Fatigue crack propagation rate as a function of  $\Delta K$  at transformation temperatures of; (○) 573 K, (●) 593 K, (△) 623 K and (▲) 643 K.

fatigue FCP: region I (the threshold region), region II (the region of stable continuum, controlled crack growth) and region III (the region when growth is largely continuum controlled but static fracture modes exert some influence) [24].

In the low  $\Delta K$  region, the fatigue crack grows at very low rate ( $da/dN < 10^{-8}$  m per cycle). The FCP behaviour clearly shows a microstructure dependence. The transformation temperature has a great effect on the FCP rate and threshold. The FCP threshold increases with an increase in the transformation temperature. At the same  $\Delta K$  level, the increase in the transformation temperature results in a significant decrease in the FCP rate.

In the higher  $\Delta K$  region, the fatigue crack grows at higher rate ( $da/dN > 10^{-8}$  m per cycle). In this regime, any effect of microstructure on the FCP rate is not obvious. That is to say, at the same  $\Delta K$  level, the difference between the FCP rates of the four microstructures is not larger than that of the FCP thresholds.

The relationship between FCP rate ( $da/dN$ ) and  $\Delta K$  level in region II can be described by using the Paris formula

$$da/dN = c(\Delta K)^m \quad (1)$$

where  $c$  and  $m$  are material specific constants.

Values of  $\Delta K$ ,  $c$  and  $m$  are shown in Table II. The values of  $m$  and  $\Delta K$  both increase with an increase in the transformation temperature. A comparison of the specimens transformed at 643 and 573 K, shows that the  $m$  value for the specimen transformed at 643 K is 10% higher than that transformed at 573 K. However the threshold value of the former is 50% higher than the latter. From Table 1, we can conclude that, although  $m$  values of the four microstructures have only small differences in general a higher  $\Delta K$  results in a higher  $m$ .

In the present study, the effects of microstructure on the thresholds have been shown by the volume fraction of austenite (FA) (given in Table 1) and of bainite (FB) ( $FB = 1 - FA$ ). The  $\Delta K$  value increases with an increase in FA and a consequent decrease in FB. In order to indicate the relative value of the effect of austenite to that of bainite on the  $\Delta K$  value a polynomial regression was used for data processing. The results give the following relation,

$$\Delta K = 38FA + 5FB, \quad (2)$$

the relative coefficient  $R = 0.98$ . For experimental data groups ( $y_i, x_{1i}, x_{2i}$ ),  $i = 1, 2, \dots, m$ , if the regression relation is  $y = b_0 + b_1x_1 + b_2x_2$ ,  $R$  is defined as

$$R = \sqrt{\frac{b_1 \left( \sum_{i=1}^m x_{1i}y_i - \frac{\sum_{i=1}^m x_{1i}}{m} \sum_{i=1}^m y_i \right) + b_2 \left( \sum_{i=1}^m x_{2i}y_i - \frac{\sum_{i=1}^m x_{2i}}{m} \sum_{i=1}^m y_i \right)}{\sum_{i=1}^m y_i^2 - \frac{(\sum_{i=1}^m y_i)^2}{m}}}$$

TABLE II  $\Delta K$ ,  $c$  and  $m$  values at various transformation temperatures

Austempering temperature (K)	$\Delta K$ (MPam <sup>1/2</sup> )	$c^*$ ( $\times 10^{-12}$ )	$m^*$
573	8.08	39.3	2.58
593	8.64	13.2	2.78
623	10.13	8.0	2.89
643	12.91	2.5	3.12

\* $m$  is a unit free constant. Unit for  $c$  is [m] [cycle<sup>-1</sup>] [(MPam<sup>1/2</sup>)<sup>-m</sup>].

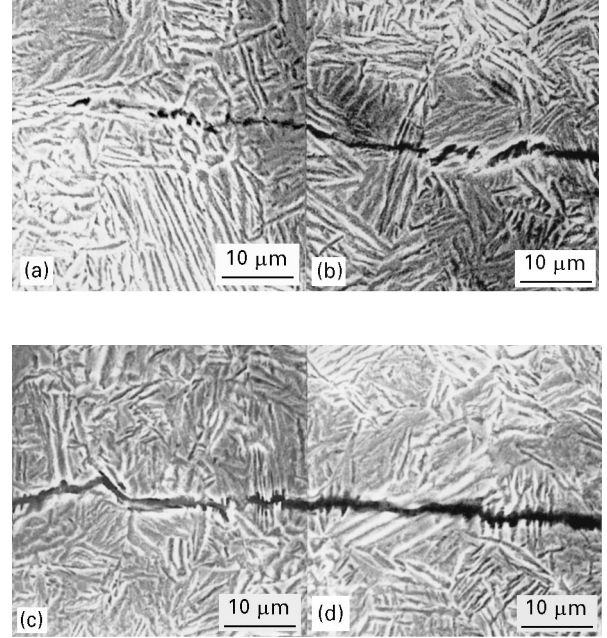


Figure 3 Fatigue crack propagation routes (a) 623 K,  $\Delta K = 9.3 \text{ MPam}^{1/2}$ ,  $da/dN = 10^{-10}$  m per cycle (b) 623 K,  $\Delta K = 10 \text{ MPam}^{1/2}$ ,  $da/dN = 3 \times 10^{-9}$  m per cycle (c) 623 K,  $\Delta K = 12 \text{ MPam}^{1/2}$ ,  $da/dN = 10^{-7}$  m per cycle (d) 623 K,  $\Delta K = 20 \text{ MPam}^{1/2}$ ,  $da/dN = 6 \times 10^{-7}$  m per cycle

It can be seen that the effect of austenite on the  $\Delta K$  value is seven times that of bainite.

### 3.2. The fatigue crack growth routes

At low  $\Delta K$  levels (threshold region), the fatigue crack grows at very low speed along phase boundaries or in the austenite films, and is contained within two or three grain sizes, as is shown in Fig. 3a. This is because the  $\Delta K$  level in this region is relatively low, and the fatigue crack cannot cut across the strong bainite lathes but instead grow along the slip plane of the austenite. In the plastic deformation region, the high deformation strengthening ability of the austenite improves the resistance to slip. Thus a fatigue crack is

hard to grow and therefore a high FCP threshold is obtained. At higher  $\Delta K$  levels (near the threshold region), the fatigue crack grows at a higher rate along a grain boundary or cuts across the bainite lathes. Its growth path is very tortuous, as is shown in Fig. 3b. An increase in  $\Delta K$  results in the enlargement of the plastic zone in the crack tip. The unhomogeneous deformation in the plastic region causes stress concentration in the grain boundary. Since the  $\Delta K$  value is still low, the crack grows along the low energy paths, such as grain boundaries. At high  $\Delta K$  levels (stable growth region), the fatigue crack grows in a straight path, as is shown in Fig. 3c. The effect of microstructure on the FCP is not obvious. These results are in agreement with earlier investigations.

#### 4. Conclusion

The microstructure has a significant effect on the FCP threshold in that the effect of austenite on the FCP threshold is seven times that of bainite. The FCP threshold of this steel increases with an increase in the volume fraction of carbon-saturated austenite. The deformation strengthening ability of the austenite has a significant effect on the FCP in the threshold region. However, no obvious effect of the microstructure on the FCP behaviour in the stable growth region could be observed.

#### References

1. H. K. D. H. BHADESHIA and D. V. EDMONDS, *Metall. Trans. A* **10A** (1979) 895.
2. *Idem*, *Acta Metall.* **28** (1980) 1265.
3. JIALIN SUN, HONGXIU LU and MOKUANG KANG, *Metall. Trans. A* **23A** (1992) 2483.
4. Y. TOMITA, *J. Mater. Sci.* **29** (1994) 2605.
5. S. J. MATAS and R. F. HEHEMANN, *Trans. Metall. Soc. AIME* **221** (1961) 179.
6. B. P. J. SANDVIK, *Metall. Trans. A* **13A** (1982) 777.
7. Y. THOMITA and T. OKAWA, *Mater. Sci. Engng.* **A172** (1993) 145.
8. SHI DEKE, LIU JUN HAI and CHENG YAO QIANG, *ibid.* **A158** (1992) 11.
9. QU JINGXIN, LUAN DAOCHENG, YANG DONGFANG and SHAO HESHENG, *J. of China University of Mining and Technology* **21** (1992) 20 (in chinese).
10. QU JINGXIN, YANG DONGFANG, LUAN DAOCHENG and SHAO HESHENG, *J. of Iron and Steel Research* **4** (1992) 53 (in Chinese).
11. QU JINGXIN, WANG HUAMING, ZHANG QING and SHAO HESHENG, *Chin. J. Met. Sci. Technol.* **8** (1992) 411.
12. H. K. D. H. BHADESHIA and D. V. EDMONDS, *Met. Sci.* **17** (1983) 411.
13. *Idem*, *ibid.* **17** (1983) 420.
14. V. T. T. MIIHKINEN and D. V. EDMONDS, *Mater. Sci. Technol.* **3** (1987) 432.
15. *Idem*, *ibid.* **3** (1987) 441.
16. QU JINGXIN, YANG DONGFANG, LUAN DONGCHENG, and SHAO HESHENG, *J. Iron Steel Research* **4** (1992) 47 (in chinese).
17. *Idem*, *Mater. for Mech. Engng* **17** (1993) 20 (in chinese).
18. QU JINGXIN and WU XIAOLI, *Heat Treat. Met.* **9** (1992) 37 (in chinese).
19. J. P. NAYLOR and P. R. KRAHE, *Metall. Trans. A* **6A** (1975) 8594.
20. Y. TOMITA and K. OKABAYASHI, *ibid.* **14A** (1983) 485.
21. D. V. EDMONDS and R. C. COCHRANE, *ibid.* **21A** (1990) 1527.
22. F. YIN, N. GU, M. KANG and W. LIU, *ibid.* **21A** (1990) 2282.
23. V. K. SAXENA, G. MALAKONDAIAH, V. M. RADHAKRISHNAN and P. R. RAO, *Scripta Metall. et Mater.* **28** (1993) 1257.
24. J. H. BULLOCH, *Int. Pres. & Piping* **54** (1993) 497.

*Received 6 February  
and accepted 17 July 1996*